East European Journal of Physics. 3. 263-270 (2023)
DOI:10.26565/2312-4334-2023-3-23 ISSN 2312-4334

FIRST-PRINCIPLES CALCULATION OF STRUCTURAL, ELECTRONIC, AND OPTICAL PROPERTIES OF CUBIC PEROVSKITE $CsPbF_3$[†]

Zozan Y. Mohammed[§], Sarkawt A. Sami[‡], Jalal M. Salih*
Department of Physics, College of Science, University of Duhok, Kurdistan Region-Iraq
[§]e-mail: zozan.abde@uod.ac; [‡]e-mail: sarkawt@uod.ac
**Corresponding Author e-mail: jalal@uod.ac*
Received February 16, 2023; revised March 7, 2023; accepted March 9, 2023

Lead halide perovskites have attracted considerable attention as one of the most promising materials for optoelectronic applications. The structural, electronic, and optical properties of the cubic perovskite $CsPbF_3$ were studied using density functional theory in conjunction with plane waves, norm-conserving pseudopotentials, and Perdew-Berg-Erzenhof flavor of generalized gradient approximation. The obtained structural parameters are a good agreement with the experimentally measured and other's theoretically predicted values. The obtained electronic band structure revealed that cubic $CsPbF_3$ has a direct fundamental band gap of 2.99 eV at point R. The calculated energy band gaps at the high symmetry points agree with the other available theoretical results. The GW method is adapted to correct the underestimated fundamental energy gap value to 4.05 eV. The contribution of the different bands was analyzed from the total and partial density of states. The electron densities show that Cs and F have strong ionic bonds, whereas Pb and F have strong covalent bonds. The optical properties of $CsPbF_3$ were calculated using the density functional perturbation theory and Kramers-Kronig relations. The wide and direct bandgap nature and the calculated optical properties imply that cubic $CsPbF_3$ can be used in optical and optoelectronic devices for high frequencies visible and low frequencies ultraviolet electromagnetic radiation.
Keywords: *$CsPbF_3$; Perovskite; Structural properties; Bandgap; Optoelectronic properties; First-principles method*
PACS: 71.15._m; 71.15.Mb; 71.20.−b; 71.20.Nr

1. INTRODUCTION

Based on first principles approaches, several computational techniques have been developed to investigate the properties of materials. Using these first principles techniques, it is possible to predict many of the physical and chemical characteristics of the condensed matter with acceptable accuracy.

Perovskites have become extremely important from both a technological and science due to their commonly observed characteristics, such as high thermoelectric power, spin-dependent transport, superconductivity, ferroelectricity, charge ordering, colossal magneto-resistance, and the interplay of magnetic, structural and optical properties [1], [2]. These materials are often employed as substrates, sensors, and catalytic electrodes in fuel cells, and they also represent interesting optoelectronics material choices [3]–[6]. Inorganic halide-based cubic perovskite structures have also been researched and shown to have excellent absorption and low reflection coefficients as used in solar cells and optoelectronic devices [7]. Besides that, the progression of the perovskite solar cells' efficiency rose by more than 6% in the range of 10 years, as a result of their lowering costs and friendly environment [8], [9].

Perovskite fluorides are widely used as antireflective and protective coatings due to their distinctive optoelectronic characteristics. They are recognized for having fast ion conduction. In $CsPbF_3$, rapid fluoride ion conduction has been recognized [10], [11]. The single crystal of $CsPbF_3$ is a useful perovskite for studies of ionic diffusion due to its chemical bonding, relatively simple crystal structure, and excellent fluorine diffusivity throughout a wide temperature range [10]. $CsPbF_3$ has a cubic perovskite (*Pm3m*), according to a preliminary analysis of the diffraction pattern at room temperature [12]. $CsPbF_3$, which has a direct bandgap and is good in optical characteristics, may be employed successfully in photonic and optoelectronic devices despite being a possible compound for high-frequency optical systems.

There have been some theoretical studies written on $CsPbF_3$, which, reported by many researchers, who has been computed the Cubic Perovskite structural, and optoelectronic properties, which used the DFT method to analyze the Kohn-Sham equations, together with the full-potential linearized augmented plane-wave (FPLAP-W) approximation within the Wu-Cohen generalized gradient approximation (GGA)[3]. [13] another researcher applied projector augmented wave (PAW) Potentials under the PBEsol functional to study the structural properties of $CsPbF_3$.

Other studies have been published, by utilizing the DFT and the PAW method with (PBE-GGA) Perdew-Burke-Ernzerhof generalized gradient approximation, which calculated bandgap in cubic phase with *Pm3m* space group and rhombohedral phase with *R3c* space group of $CsPbF_3$ and polarizability, Rashba parameters for optoelectronic applications [14].

Also, first principle calculations have been used to calculate the structural and optoelectronic properties of $CsPbF_3$-yIy (y = 0, 1, 2), and the exchange and correlation were handled by both the GGA and HSE06 functionals [15].

Also, the structural and optoelectronic properties of Cs-based fluoroperovskites $CsMF_3$ (M = Ge, Sn or Pb) were studied and used (DFT) method with (GGA-PBE)[16].

[†] ***Cite as:*** Z.Y. Mohammed, S.A. Sami, J.M. Salih, East Eur. J. Phys. 3, 263 (2023), https://doi.org/10.26565/2312-4334-2023-3-23

The aim of this study is the investigation of the structural, electronic, and optical properties of cubic perovskite $CsPbF_3$ theoretically in the context of (DFT) by using ab initio calculations, by ABINIT code. Accordingly, all calculations were conducted using the plane waves with the norm-conserving pseudopotentials (PW-PP) schemes. Specifically, we compute a Kohn Sham gap in the frame of a known (PBE-GGA). Furthermore, Green's function and screened Coulomb-interaction (GW) approximations have been used to update band gap values (Eg). The current study will present a better aid in understanding the possible applications of the chosen candidate, $CsPbF_3$.

2. COMPUTATION DETAIL

In the present work, the structural, electronic, and optical characteristics of the cubic perovskite $CsPbF_3$ have been computed using the DFT framework. The wave functions were expanded in plane waves (PWs) as basis sets. The interaction between the valence electrons and ions was accounted for by the optimized norm-conserving Vanderbilt pseudopotentials [17]. The exchange-correlation term in the Kohn-Sham equations was treated by the Perdew-Berg-Erzenhof flavor of generalized gradient approximation (PBE-GGA). All calculations were performed by the ABINIT code [18]–[20]. A cubic perovskite structure, its general formula is ABX_3, has five atoms per unit cell, and belongs to the space group Pm–3m (#221). The locations of the five atoms are considered as follows: A, B, and the three X atoms occupy 0.0 0.0 0.0, 0.5 0.0 0.5, 0.5 0.5 0.0, 0.5 0.0 0.5 and 0.0 0.5 0.5, respectively (Figure 1).

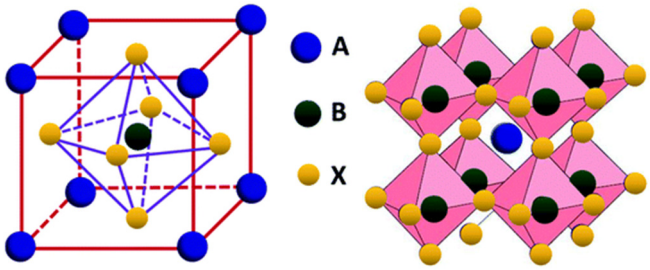

Figure 1. The cubic perovskite structure ABX_3 [21]

Convergence calculations have resulted in the cut-off energy of 1632.68 eV and (336) k points, which correspond to the 14×14×14 k-point grid of Monkhorst–Pack. The structural geometry was optimized depending on the achievement of atomic coordinates relaxation. The resulting optimized values of *a* and relaxed atomic coordinates were exploited to calculate band structure. They have also been used in the calculations of the total density of states (TDOS), the partial density of states (PTDOS), and optical properties. To correct the well-known DFT underestimation of the energy gap value [22], the GW approximation on energies and wavefunctions was carried out.

Optical properties have been calculated using density functional perturbation theory (DFPT) [23] and Kramers-Kronig relations[24]. The later were used to obtain the real and imaginary parts of the dielectric function. In addition, the refractive index, extinction coefficient, reflectivity, and absorption coefficient of the cubic $CsPbF_3$ for incident photons of energies from 0.08 eV to 40 eV have been computed. In calculating the optical properties, the interaction between the valence electrons and ions was accounted for by the norm-conserving, separable, dual-space Gaussian-type pseudopotentials by Goedecker, Teter, and Hutter (GTH) [25], [26].

3. RESULTS AND DISCUSSION

Structural properties

The optimization calculation produced the values of total energy, E_{tot}, and pressure, P, for various values of *a* (hence, unit cell volume). Figure (2) shows the total energy E_{tot} plot versus lattice constant *a*, from which the optimized value of *a* for the cubic $CsPbF_3$ was taken, see Table 1. The pressure P against the volume of the unit cell is plotted in Figure (3), from which the unit cell volume at P = 0, V_o, was calculated, see Table (1).

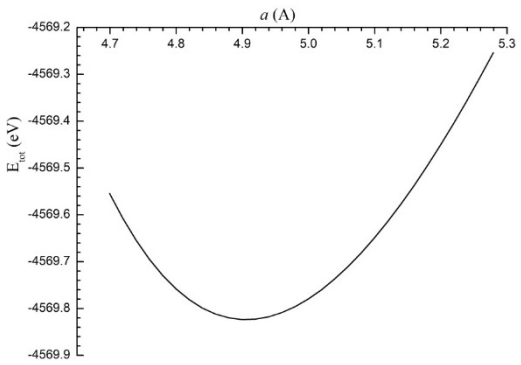

Figure 2. Total energy, E_{tot}, versus lattice parameter, *a*, of cubic $CsPbF_3$

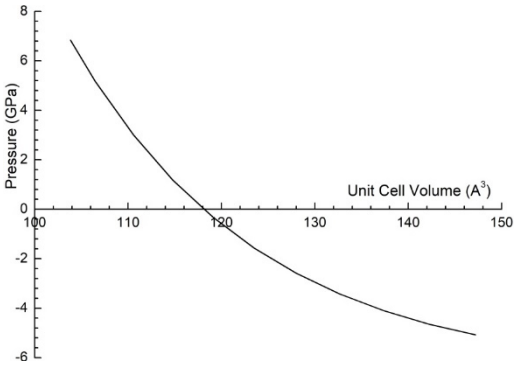

Figure 3. Pressure versus the corresponding unit cell volume of cubic $CsPbF_3$

Table 1. Optimized structural properties of cubic $CsPbF_3$ calculated using PBE-GGA flavor

Parameter	Present work	Theoretical	Experimental
a (A)	4.9051866	4.80652[c],4.800[a], 4.777[b],4.773[f],4.653[b],4.90[h]	4.795[a,e] 4.774[b], 4.7748[f,g]
E_{tot} (eV)	–4569.8241	–60201.5279 [b]	n.a*
B_o (GPa)	39.013	52 [b], 27.19 [d],39.035[f]	n.a
B_o`	4.811	5.11[b], 5.765[f]	n.a
V_o (A^3)	118.022986	109.041[b],116.02[f]	108.864 [b, g]
Bond length (A)			
Cs-F	3.469	3.98[b]	n.a
Pb-F	2.453	2.33[b]	n.a

* Here and below the notation, "n.a." stands for "not available".
[a] Ref. [29], [b] Ref [3], [c] Ref. [14], [d] Ref. [30], [e] Ref. [10], [f] Ref. [15], [g] Ref. [12].[h] Ref.[16]

The change of pressure P with the unit cell volume V of the cubic $CsPbF_3$ was fitted to the second-order Birch-Murnaghan equation of state [27]:

$$P(V) = \frac{3B_0}{2}\left[\left(\frac{V_0}{V}\right)^{7/3} - \left(\frac{V_0}{V}\right)^{5/3}\right]\left[1 + \frac{3}{4}(B_o' - 4)\left\{\left(\frac{V_0}{V}\right)^{2/3} - 1\right\}\right], \quad (1)$$

where B_o and B_o' are the zero-pressure value of bulk modulus and its pressure derivative, respectively.

From the fitting, the values of B_o and B_o' were obtained and they are given in Table (1). The length of the bonds Cs-F and Pb-F were also calculated and are given also in Table (1). The results of the bond length calculation show that the bond Cs-F is longer than the bond Pb-F. Referring to the electronegativity of atoms [28], this agrees with the fact that the electronegativity difference between atoms Cs and F is larger than that between Pb and F. Thus, all optimized structural properties, calculated with GGA-PBE flavor, were obtained and are listed in Table (1).

The calculated structural properties agree well with those from experiments as well as other theoretical investigations that have been done utilizing various DFT implementations, see Table (1).

Electronic properties

The electronic properties of the cubic $CsPbF_3$ were investigated through the computation of the band structure, TDOS, and PDOS. The energy of the bands was computed at the high symmetry k-points from point R to Γ along the symmetry lines R–Γ–X–M– Γ. The computed band structure is plotted in Figure (4). The figure reveals that both the minimum of the bottom conduction band (BCB), band 23, and the maximum of the top valence band (TVB), band 22, are located at the symmetry point R. That is, the cubic $CsPbF_3$ has a direct fundamental energy band gap at the symmetry point R, E_g^{R-R}. The energy gaps at k points R, Γ, X and M were calculated and are given in Table (2) along with other available theoretical results.

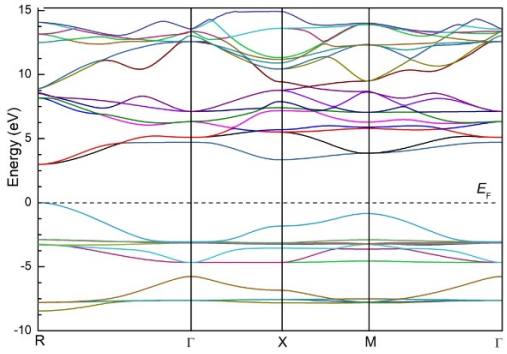

Figure 4. Band structure of cubic $CsPbF_3$

Table 2. Computed energy gaps in (eV) at some high symmetry points in the PBE-GGA approach. Results of other theoretical works are also given.

$CsPbF_3$	Eg^{R-R}	$Eg^{\Gamma-\Gamma}$	Eg^{X-X}	Eg^{M-M}
Present work	2.99336	7.77865	5.18326	4.71271
Theoretical works	2.55 [a, d], 2.62[c],2.642 [d], 2.98[e]	n.a.	5.9 [b]	5.7 [b]

[a] Ref. [29], [b] Ref. [3], [c] Ref. [14], [d] Ref. [15], [e] Ref.[16].

The present work reveals that the PBE-GGA value of the fundamental energy gap, E_g^{R-R}, is 2.99336 eV, see Table (2). It is also clear from Table (2) that the present calculated energy band gaps of the cubic $CsPbF_3$ using the PBE-GGA method are consistent with other available theoretical studies. The calculated E_g^{R-R} value using PBE-GGA suffers from the well-known problem of the DFT's underestimation of the energy gap. To correct this underestimated value of

E_g^{R-R}, the GW method on energies and wavefunctions was used. The obtained corrected value of E_g^{R-R} was 4.052 eV, which agrees well with other available theoretical results, see Table (3). Unfortunately, no experimental value is available on the fundamental band gap of the cubic $CsPbF_3$.

Table 3. Fundamental band gap E_g^{R-R} computed using PBE-GGA and GW along with results of other works

$CsPbF_3$	E_g^{R-R} (eV)		
	PBE-GGA value	Actual value	
		GW	Other methods
Present work	2.99336	4.052	---
Theoretical	2.98[f], 2.55 [e, d], 2.62[c], 2.642 [d]	n.a	3.8[a], 3.92[b], 2.42[c],2.642[d], 3.707[d],
Experimental	n.a	n.a	

[a] Ref. [3],[b] Ref. [30],[c] Ref. [14],[d] Ref. [15],[e] Ref. [29],[f] Ref. [16].

The electronic properties can be further elaborated in terms of the density of states. That is, understanding the electronic band structure becomes more comprehensive when enlightened by DOS. For this purpose, the TDOS and PDOS for the cubic $CsPbF_3$ were calculated and are presented in Figure (5) and Figure (6), respectively. The PDOS is essential to know the contributions of different atomic states to the bands.

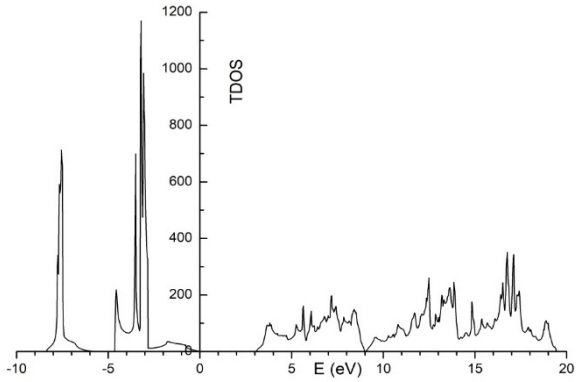

Figure 5. Total density of state (TDOS) of cubic $CsPbF_3$

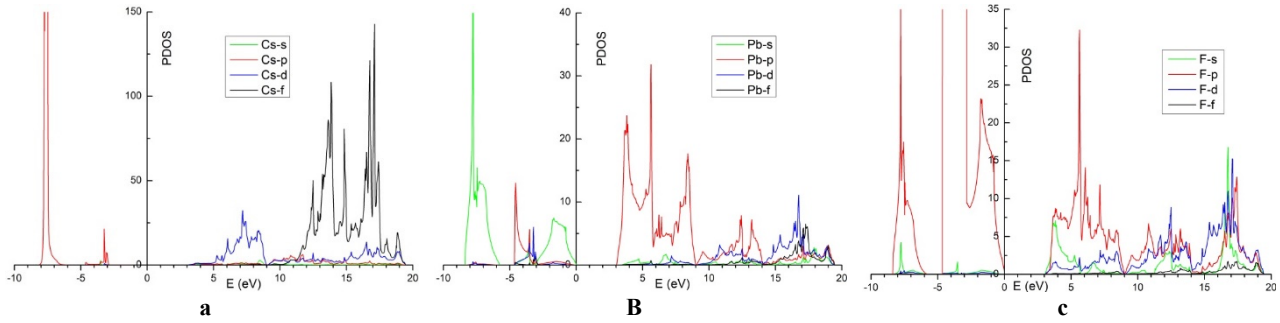

Figure 6. Partial density of states (PDOS) for the atoms (a) Cs, (b) Pb, and (c) F

The band structure of the cubic $CsPbF_3$ from –10 eV to 20 eV (looking at TDOS, Fig. (5) is divided into three dense VB regions and three dense CB regions. The three VB regions are in the energy ranges –8.5 eV to –6.0 eV, –4.7 eV to -2.8 eV, and –2.8 eV to 0 eV. The three CB regions boundaries are 3 eV, 9 eV, 14 eV, and 20 eV. It is interesting to investigate the amount of contribution of the atomic orbitals of the three atoms to each of these six regions. However, because of their role in the optical response, only the upper region of VB and the lower region of CB will be investigated. To realize the amount of the contribution of each of the atoms Cs, Pb, and F to the upper region, ~ (–2.8 to 0) eV, of VB, the full PDOS of the three atoms corresponding to the VB have been plotted alongside, see Fig. (7).

It is clear from Fig. (7) that the bands in this range, ~ (–2.8 to 0) eV, arise mainly from the F-p orbital. The Pb-s orbital contribution is small, namely, one-third of F-p, the contribution of Pb-p is very small, and Pb-d and F-s contributions are almost insignificant. It is clear from Fig. (6) that the lower region of the CB, (14 to 200) eV, arises mainly from Cs-d, Pb-p, and F-p orbitals, which nearly contribute equally, while the contribution of F-s is less, namely, about one fifth. The contribution of F-d is small, that of Cs-s, Pb-d, and Pd-f are very small and Cs-p, Cs-f, and F-s contribute almost insignificantly.

Figures (5) – (7) reveal that the top most four states in VB, above –4.7 eV, arise mainly from F-p orbital and much less from Pb-s. The bottom most nine states of CB, below 9 eV, arise mainly from the orbitals Cs-d, Pb-p, and F-p, which equally contribute. It is also clear that the lower edge of the fundamental band gap is determined by the F-p orbital,

Fig. (7), while the upper edge of the fundamental band gap arises from the Pb-p orbital, Fig. (6b). This implies that the fundamental band gap arises from the higher occupied orbital of the F atom and the higher occupied orbital of Pb, which are F-$2p^5$ and Pb-$6p^2$, respectively. Accordingly, one realizes that the fundamental band gap can be tuned by changing the atoms F and/or Pb, provided the new structure be stable.

In summary, see Fig. 6, the formation of VB is mostly due to the contribution of the s state of Pb and p states of Cs and F, while CB is mostly due to the contributions of the f state of Cs and p states of Pb and F. The calculated DOS is in good agreement with the previous theoretical results [3], [15].

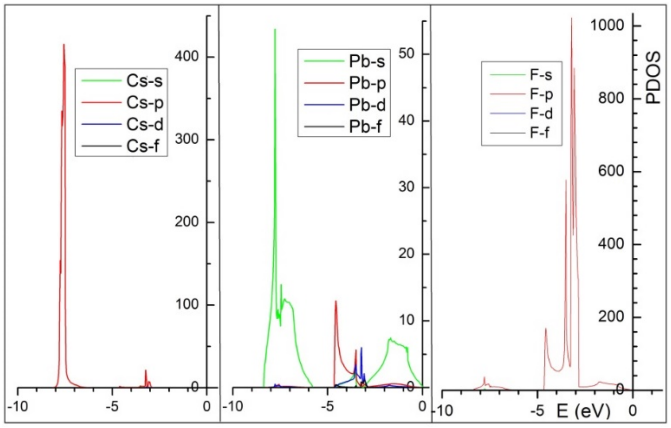

Figure 7. Partial density of states (PDOS) of VB for the atoms (a) Cs, (b) Pb, and (c) F.

Optical properties

To predict a material's possibilities for use in photovoltaic devices, the investigation of its optical properties is crucial. The most important frequency-dependent optical properties are the refractive index n(ω), extinction coefficient k(ω), reflectivity R(ω), and absorption coefficient α(ω). These characteristics can be calculated using [31]:

$$n(\omega) = \left[\frac{\varepsilon_1(\omega)}{2} + \frac{\sqrt{\varepsilon_1(\omega)^2+\varepsilon_2(\omega)^2}}{2}\right]^{1/2} \tag{2}$$

$$k(\omega) = \left[\frac{\varepsilon_1(\omega)}{2} - \frac{\sqrt{\varepsilon_1(\omega)^2+\varepsilon_2(\omega)^2}}{2}\right]^{1/2} \tag{3}$$

$$R(\omega) = \left|\frac{\sqrt{\varepsilon(\omega)}-1}{\sqrt{\varepsilon(\omega)}+1}\right|^2 \tag{4}$$

and

$$\alpha(\omega) = \frac{4\pi k(\omega)}{\lambda} \tag{5}$$

respectively, where $\varepsilon_1(\omega)$ and $\varepsilon_2(\omega)$ are the real and imaginary components of the dielectric function ε:

$$\varepsilon(\omega) = \varepsilon_1(\omega) + i\varepsilon_2(\omega) \tag{6}$$

The real component ε_1 of the dielectric function indicates the retaining ability of the material while the imaginary component ε_2 determines its absorptive ability. As much as solar cells are concerned, ε_1 determines the ability of the cell to store energy, and ε_2 determines its absorption limitations and, thus, capability to gain energy [32].

It is clear from Eqs. (2)–(5) that if the real and imaginary components of the dielectric function are known, it is possible to compute those optical properties. Using DFPT [18] and Kramers-Kronig relations [33], the real and imaginary components of the dielectric function were computed for incident photon energies from 0.08 eV to 40 eV. Then, the frequency-dependent optical properties were calculated using Eqs. (2)–(5). The computed real and imaginary components of the dielectric function, n, k, R, and α spectra are shown in Figure (8).

Figure (8a) reveals that the value of the zero-frequency limit $\varepsilon_1(0)$, known also as the static dielectric constant, for cubic $CsPbF_3$ is 3.14. The knowledge of the value of the static dielectric constant is important in optoelectronic and photovoltaic technology. The higher the $\varepsilon_1(0)$ value, the greater the potentiality of the material for designing optoelectronic devices [34]. The figure shows that starting from the zero-frequency limit $\varepsilon_1(0)$, $\varepsilon_1(\omega)$ begins to rise and, after a few peaks, reaches its maximum value of 5.42 at 4.65 eV beyond which gradually declines passing through many peaks and becoming negative in the energy range (15.10-17.71) eV. Thus, the cubic $CsPbF_3$ has a dielectric behavior ($\varepsilon_1(\omega) > 0$) in response to the most investigated photon spectra except for the energy range 15.10 – 17.71 eV for which it has a metallic characteristic ($\varepsilon_1(\omega) < 0$). The negative $\varepsilon_1(\omega)$ in an energy range indicates the attenuation of the incident photon in that range, thus, a metallic behavior of the material [35].

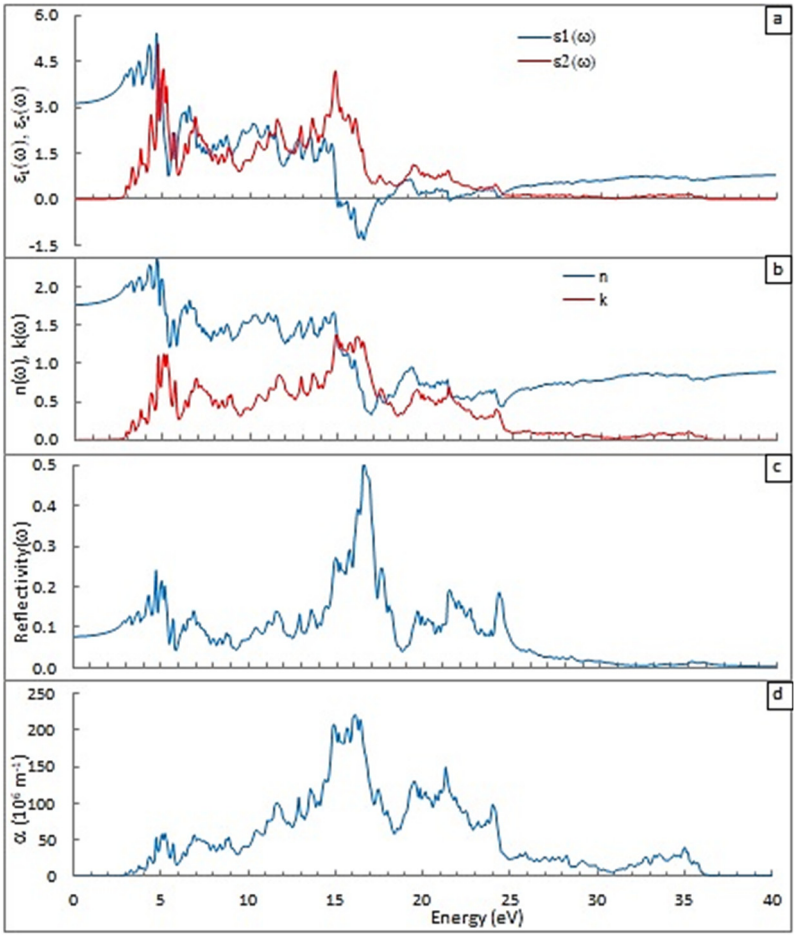

Figure 8. Optical properties versus the energy of cubic $CsPbF_3$: (a) Real ε_1 and imaginary ε_2 parts of the dielectric function, (b) Refractive index n and extinction coefficient k, (c) Reflectivity R, and (d) Absorption coefficient α.

The $\varepsilon_2(\omega)$ illustrates the absorption of incoming radiation impinging at the surface, and the excellent optical materials absorb the incoming photons, almost entirely, within the top surface. Its values are compatible with those estimated from the electronic band structures and are closely connected to the optical band gap.

It is noticed from Figure (8a) that the threshold point in the spectrum of $\varepsilon_2(\omega)$ is nearly at 2.9 eV. This threshold corresponds to the transition from the VB state that arises from the orbitals F-2p and Pb-6s to the CB state that arises from the Pb-6p orbital, see Fig. (6). The value of the threshold is solely determined by the fundamental band gap. The figure shows that starting from the threshold, $\varepsilon_2(\omega)$ starts increasing and, after a few peaks, reaches its maximum value of 5.07 at 4.74 eV, then, passing through many peaks, reaches another high-value peak of 4.20 at 14.86 eV beyond which it decreases and almost vanishes beyond 24.00 eV.

Figure (8b) shows that the variation of the refractive index $n(\omega)$ and extinction coefficient $k(\omega)$ follow the same pattern as ε_1 and ε_2, respectively. The $n(\omega)$ increases from its zero-frequency limit n(0), 1.77, and reaches its maximum value of 2.38 at 4.65 eV. The $k(\omega)$ spectrum indicates that the maximum extinction coefficient is 1.37 and occurs at 14.94 eV. Beyond 24.41 eV, $k(\omega)$ almost vanishes. For incident photons having energies greater than 15.67 eV, the refractive index $n(\omega)$ becomes less than one which implies that the group velocity, $\upsilon_g = c/n$, is greater than the speed of light c. The conversion from $n > 1$ to $n < 1$ occurs at the same energy at which $\varepsilon_1(\omega)$ has the largest negative value, see Fig. (8a and 8b).

Figure (8c) represents the computed frequency-dependent reflectivity $R(\omega)$. The figure reveals that the zero-frequency limit of reflectivity, R(0), is about 0.08. The figure shows that starting from the zero-frequency limit R(0), $R(\omega)$ begins to rise and, after a few peaks, reaches its maximum value of 0.50 at 16.57 eV then decreases passing through many peaks and approaches zero beyond 30 eV, that is, cubic $CsPbF_3$ becomes almost transparent to photons of energies higher than 30 eV.

One can notice, in Fig. (8a – 8c), that the maximum negative value of $\varepsilon_1(\omega)$ and transition of $n(\omega)$ value to less than one, both, occur at the same photon energy, ~16.5 eV, and coincide with the maximum value of $R(\omega)$. This implies that, at that energy, cubic $CsPbF_3$ becomes superluminal, a common behavior in perovskites [36], [37].

The computed absorption coefficient $\alpha(\omega)$ is presented in Fig. (8d). $\alpha(\omega)$ spectrum predicts how many photons of various energies are absorbed, thus, is directly connected to the fundamental energy gap. The photons with energies lower than the fundamental energy gap are transmitted, while photons with equal and higher energies are absorbed. Figure (8d)

shows that the absorption starts around 2.99 eV and then increases to its maximum value of 220.23×10^6 m^{-1} at 16.16 eV. Figures (8a) and (8d) reveal that absorption is higher for energies at which $\varepsilon_1(\omega)$ is negative and maximum absorption occurs where $\varepsilon_1(\omega)$ has a maximum negative value. The significant values of $\alpha(\omega)$, see Fig. (8d), cover a wide range of energy, namely, about (2.9 – 36.5) eV and, thus, for high energies visible light and low ultraviolet, the cubic $CsPbF_3$ perovskite is a promising material for a variety of optical and optoelectronic devices.

CONCLUSIONS

The structural, electronic, and optical properties of cubic $CsPbF_3$ have been investigated by using first-principles computations, namely, the DFT with the PBE-GGA flavor as the exchange-correlation energy. The structural properties, band structure, and total and partial density of states were calculated. The GW approximation was implemented to correct the underestimated energy band gap. The optical properties were also computed using Kramer–Kronig relations.

The calculated structural characteristics, such as lattice constant, bond length, bulk modulus, and its pressure derivative, agree well with other theoretical and experimental findings. The calculated length of the bonds Cs-F and Pb-F are consistent with the electronegativity of the three atoms. The computed band structure reveals that cubic $CsPbF_3$ has a direct fundamental energy band gap that is located between band 22 and band 23 at the symmetry point R. The calculated energy band gaps at the high symmetry points R, Γ, X and M are in good agreement with those of other theoretical studies. The calculated value of the fundamental energy band gap, 4.025 eV, suggests that cubic $CsPbF_3$ is a wide band gap semiconductor.

The real and imaginary parts of the dielectric function, refractive index, extinction coefficient, reflectivity, and absorption coefficient were calculated for incident photon energies from 0.08 eV to 40 eV. In the spectrum of the imaginary part of the dielectric function, different characteristics are seen, mostly as a result of the transitions from the VB states that arise from Cs-p and F-p orbitals to unoccupied states in the CB. The spectrum of the real part of the dielectric function revealed that cubic $CsPbF_3$ has a metallic behavior in response to the incident photon energies from 15.10 eV to 17.71 eV.

The calculated absorption coefficient is appreciable in the high-frequency visible and low-frequency ultraviolet regions, thus, indicating the feasibility of cubic $CsPbF_3$ to be used in optoelectronic devices for such regions of electromagnetic radiation.

ORCID

Jalal M. Salih, https://orcid.org/0000-0002-9587-3351

REFERENCES

[1] C. Weeks, and M. Franz, "Topological insulators on the Lieb and perovskite lattices," Phys. Rev. B - Condens. Matter Mater. Phys. **82**(8), 1-5 (2010), https://doi.org/10.1103/PhysRevB.82.085310
[2] A.S. Moskvin, A.A. Makhnev, L.V. Nomerovannaya, N.N. Loshkareva, and A.M. Balbashov, "Interplay of p-d and d-d charge transfer transitions in rare-earth perovskite manganites," **82**(3), 035106 (2018), https://doi.org/10.1103/PhysRevB.82.035106
[3] G. Murtaza, I. Ahmad, M. Maqbool, H.A.R. Aliabad, and A. Afaq, "Structural and optoelectronic properties of cubic CsPbF3 for novel applications," Chinese Phys. Lett. 28(11), 117803 (2011), https://doi.org/10.1088/0256-307X/28/11/117803.
[4] J. Burschka, N. Pellet, S.-J. Moon, R. Humphry-Baker, P. Gao, M.K. Nazeeruddin, and M. Grätzel, "Sequential deposition as a route to high-performance perovskite-sensitized solar cells," Nature, **499**(7458), 316-319 (2013), https://doi.org/10.1038/nature12340
[5] S.D. Stranks, G.E. Eperon, G. Grancini, C. Menelaou, M.J.P. Alcocer, T. Leijtens, L.M. Herz, et al., "Electron-hole diffusion lengths exceeding 1 micrometer in an organometal trihalide perovskite absorber," Science (80)., **342**(6156), 341-344 (2013), https://doi.org/10.1126/science.1243982
[6] J. Duan, Y. Zhao, X. Yang, Y. Wang, B. He, and Q. Tang, "Lanthanide Ions Doped CsPbBr3 Halides for HTM-Free 10.14%-Efficiency Inorganic Perovskite Solar Cell with an Ultrahigh Open-Circuit Voltage of 1.594 V," Adv. Energy Mater. **8**(31), 1802346 (2018), https://doi.org/10.1002/aenm.201802346
[7] M. Roknuzzaman, K.K. Ostrikov, H. Wang, A. Du, and T. Tesfamichael, "Towards lead-free perovskite photovoltaics and optoelectronics by ab-initio simulations," Sci. Rep. **7**(1), 14025 (2017), https://doi.org/10.1038/s41598-017-13172-y
[8] A. Kojima, K. Teshima, Y. Shirai, and T. Miyasaka, "Organometal halide perovskites as visible-light sensitizers for photovoltaic cells," J. Am. Chem. Soc. **131**(17), 6050 (2009), https://doi.org/10.1021/ja809598r
[9] F. Sahli, J. Werner, B.A. Kamino, M. Bräuninger, R. Monnard, B. Paviet-Salomon, L. Barraud, et al., "Fully textured monolithic perovskite/silicon tandem solar cells with 25.2% power conversion efficiency," Nat. Mater. **17**(9), 820-826 (2018), https://doi.org/10.1038/s41563-018-0115-4
[10] V.M. Bouznik, Yu.N. Moskvich, and V.N. Voronov, "Nuclear Magnetic Resonance Study Of "F Motion In CssPbF," Chem. Phys. Lett. **37**(3), 464-467 (1976), https://doi.org/10.1016/0009-2614(76)85014-2
[11] A.V Chadwick, J.H. Strange, G.A. Ranieri, and M. Terenzi, "Studies of ionic motion in perovsmite fluorides," Solid State Ionics, **9**, 555-558 (1983), https://doi.org/10.1016/0167-2738(83)90294-1
[12] P. Berastegui, S. Hull, and S.-G. Eriksson, "A low-temperature structural phase transition in CsPbF 3," J. Phys. Condens. Matter, **13**(22), 5077 (2001), https://doi.org/10.1088/0953-8984/13/22/305
[13] E.H. Smith, N.A. Benedek, and C.J. Fennie, "Interplay of Octahedral Rotations and Lone Pair Ferroelectricity in CsPbF3," Inorg. Chem. **54**(17), 8536-8543 (2015), https://doi.org/10.1021/acs.inorgchem.5b01213
[14] P. Bhumla, D. Gill, S. Sheoran, and S. Bhattacharya, "Origin of Rashba spin-splitting and strain tunability in ferroelectric bulk CsPbF3," J. Phys. Chem. Lett. **12**(39), 9539-9546 (2021), https://doi.org/10.1021/acs.jpclett.1c02596
[15] A. Amudhavalli, R. Rajeswarapalanichamy, R. Padmavathy, and K. Iyakutti, "Electronic structure and optical properties of CsPbF3-yIy (y = 0, 1, 2) cubic perovskites," Acta Phys Pol A, **139**(6), 692-697 (2021), https://doi.org/10.12693/APHYSPOLA.139.692

[16] Y. Selmani, H. Labrim, M. Mouatassime, and L. Bahmad, "Structural, optoelectronic and thermoelectric properties of Cs-based fluoroperovskites CsMF3 (M = Ge, Sn or Pb)," Mater. Sci. Semicond. Process. **152**, 107053 (2022), https://doi.org/10.1016/j.mssp.2022.107053
[17] D.R. Hamann, "Optimized norm-conserving Vanderbilt pseudopotentials," Phys. Rev. B, **88**(8), 085117 (2013), https://doi.org/10.1103/PhysRevB.88.085117
[18] X. Gonze, B. Amadon, P.-M. Anglade, J.-M. Beuken, F. Bottin, P. Boulanger, F. Bruneval, and D. Caliste, *et al.*, "ABINIT: First-principles approach to material and nanosystem properties," Comput. Phys. Commun. **180**(12), 2582-2615 (2009), https://doi.org/10.1016/j.cpc.2009.07.007
[19] X. Gonze, F. Jollet, F. A. Araujo, D. Adams, and B. Amadon, "Recent developments in the ABINIT software package," Comput. Phys. Commun. **205**, 106-131 (2016), https://doi.org/10.1016/j.cpc.2016.04.003
[20] The ABINIT Group, maintained by Jean-Michel Beuken, https://www.abinit.org/
[21] Z. Yi, N. H. Ladi, X. Shai, H. Li, Y. Shen, and M. Wang, "Will organic-inorganic hybrid halide lead perovskites be eliminated from optoelectronic applications?," Nanoscale Adv. **1**(4), 1276-1289 (2019), https://doi.org/10.1039/c8na00416a
[22] B.M. Ilyas, and B.H. Elias, "Theoretical Study of the Structural, Elastic, Electronic, Optical and Thermodynamic Properties of CsXCl3 (X = Pb, Cd) under Pressure," Phys. B Condens. Matter, **S0921-4526**(16), 30587 (2016), https://doi.org/10.1016/j.physb.2016.12.019
[23] S. Sharma, and C. Ambrosch-Draxl, "Second-harmonic optical response from first principles," Phys. Scr. T, **T109**, 128 (2004), https://doi.org/10.1238/Physica.Topical.109a00128
[24] L.A. Collins *et al.*, "Dynamical and optical properties of warm dense hydrogen," Phys. Rev. B, **63**(18), 184110 (2001), https://doi.org/10.1103/PhysRevB.63.184110
[25] S. Goedecker, and M. Teter, "Separable dual-space Gaussian pseudopotentials," Phys. Rev. B, **54**(3), 1703 (1996), https://doi.org/10.1103/PhysRevB.54.1703
[26] C. Hartwigsen, S. Goedecker, and J. Hutter, "Relativistic separable dual-space Gaussian pseudopotentials from H to Rn," Phys. Rev. B, **58**(7), 3641 (1998), https://doi.org/10.1103/PhysRevB.58.3641
[27] F. Birch, "Finite elastic strain of cubic crystals," Phys. Rev. **71**(11), 809-824 (1947), https://doi.org/10.1103/PhysRev.71.809
[28] R.1. K. H. James E. Huheey, Ellen A. Keiter, and Collins, "lnorganic Chemistry: Principles of Structure and Reactivity," Annu. Rev. Psychol. **8**(4), 257-271 (1993), http://www.ncbi.nlm.nih.gov/pubmed/8434894
[29] L.Q. Jiang, J.K. Guo, H.B. Liu, M. Zhu, X. Zhou, P. Wu, and C.H. Li, "Prediction of lattice constant in cubic perovskites," J. Phys. Chem. Solids, **67**(7), 1531-1536 (2006), https://doi.org/10.1016/j.jpcs.2006.02.004
[30] Q. Mahmood, M. Hassan, M. Rashid, B. U. Haq, and A. Laref, "The systematic study of mechanical, thermoelectric and optical properties of lead based halides by first principle approach," Phys. B Condens. Matter, **571**, 87-92 (2019), https://doi.org/10.1016/j.physb.2019.06.061
[31] K.E. Babu, A. Veeraiah, D.T. Swamy, and V. Veeraiah, "First-principles study of electronic and optical properties of cubic perovskite CsSrF," Mater. Sci. Pol. **30**(4), 359-367 (2012), https://doi.org/10.2478/s13536-012-0047-7
[32] N.A. Abdulkareem, "First principle study of structural, electronic and optical behaviour of $CsPbX_3$ (X= Br, Cl, I) under hydrostatic pressure," University of Zakho Zakho, Kurdistan region-Iraq, 2011.
[33] L.A. Collins *et al.*, "Dynamical and optical properties of warm dense hydrogen," Phys. Rev. B - Condens. Matter Mater. Phys. **63**(18), 184110 (2001), https://doi.org/10.1103/PhysRevB.63.184110
[34] S.K. Mitro, M. Saiduzzaman, T.I. Asif, and K.M. Hossain, "Band gap engineering to stimulate the optoelectronic performance of lead-free halide perovskites RbGeX 3 (X = Cl, Br) under pressure," J. Mater. Sci. Mater. Electron. **33**(17), 13860-13875 (2022), https://doi.org/10.1007/s10854-022-08318-2
[35] B. Xu, X. Li, J. Sun, and L. Yi, "Electronic structure, ferroelectricity and optical properties of CaBi2Ta2O9," Eur. Phys. J. B, **66**, 483-487 (2008), https://doi.org/10.1140/epjb/e2008-00461-9
[36] L.J. Wang, A. Kuzmich, and A. Dogariu, "Gain-assisted superluminal light propagation," Nature, **406**(6793), 277-279 (2000), https://doi.org/10.1038/35018520
[37] N.P. Bigelow, and C.R. Hagen, "Comment on 'observation of superluminal behaviors in wave propagation,'" Phys. Rev. Lett. **87**(5), 59401-1 (2001), https://doi.org/10.1103/PhysRevLett.87.059401

ПЕРШОПРИНЦИПИ РОЗРАХУНКУ СТРУКТУРНИХ, ЕЛЕКТРОННИХ І ОПТИЧНИХ ВЛАСТИВОСТЕЙ КУБІЧНОГО ПЕРОВСКІТУ $CsPbF_3$

Зозан Ю. Мохаммед, Саркаут А. Самі, Джалал М. Саліх
Департамент фізики, Науковий коледж, Університет Духок, Курдистан, Ірак

Перовскіти галогенідів свинцю привернули значну увагу як один із найбільш перспективних матеріалів для оптоелектронних застосувань. Структурні, електронні та оптичні властивості кубічного перовскіту $CsPbF_3$ були вивчені з використанням теорії функціоналу густини в поєднанні з плоскими хвилями, псевдопотенціалами, що зберігають норму, і узагальненим градієнтним наближенням Пердью-Берг-Ерценгофа. Отримані структурні параметри добре узгоджуються з експериментально виміряними та іншими теоретично прогнозованими значеннями. Отримана електронна структура зон показала, що кубічний $CsPbF_3$ має пряму фундаментальну заборонену зону в точці R 2,99 еВ. Розраховані енергетичні заборонені зони в точках високої симетрії узгоджуються з іншими доступними теоретичними результатами. Метод GW адаптовано для корекції заниженого значення фундаментальної енергетичної щілини до 4,05 еВ. Внесок різних смуг аналізувався з повної та часткової щільності станів. Електронна густина показує, що Cs і F мають міцні іонні зв'язки, тоді як Pb і F мають міцні ковалентні зв'язки. Оптичні властивості $CsPbF_3$ розраховано з використанням теорії збурень функціоналу густини та співвідношень Крамерса-Кроніга. Широка та пряма заборонена зона та розраховані оптичні властивості означають, що кубічний $CsPbF_3$ можна використовувати в оптичних та оптоелектронних пристроях для високочастотного видимого та низькочастотного ультрафіолетового електромагнітного випромінювання.

Ключові слова: *$CsPbF_3$; перовскіт; структурні властивості; заборонена зона; оптоелектронні властивості; метод першопринципів*